

Manuscript prepared for Atmos. Chem. Phys.
with version 4.2 of the L^AT_EX class copernicus.cls.
Date: 28 June 2013

Evaluation of GEOS-5 Sulfur Dioxide Simulations during the Frostburg, MD 2010 Field Campaign.

V. Buchard^{1,2}, A.M. da Silva¹, P. Colarco³, N. Krotkov³, R.R. Dickerson^{4,5}, J.W. Stehr⁴, G. Mount⁶, E. Spinei⁶, H.L. Arkinson⁴, and H. He⁴

¹Global Modeling and Assimilation Office, NASA Goddard Space Flight Center, Greenbelt, MD, USA

²Universities Space Research Association, GESTAR, Columbia, MD, USA

³Atmospheric Chemistry and Dynamics Lab, NASA Goddard Space Flight Center, Greenbelt, MD, USA

⁴Department of Atmospheric and Oceanic Science, University of Maryland, College Park, MD, USA

⁵Department of Chemistry, University of Maryland, College Park, MD, USA

⁶Laboratory for Atmospheric Research, Washington State University, Pullman, WA, USA

Abstract. Sulfur dioxide (SO₂) is a major atmospheric pollutant with a strong anthropogenic component mostly produced by the combustion of fossil fuel and other industrial activities. As a precursor of sulfate aerosols that affect climate, air quality, and human health, this gas needs to be monitored on a global scale. Global climate and chemistry models including aerosol processes along with their radiative effects are important tools for climate and air quality research. Validation of these models against in-situ and satellite measurements is essential to ascertain the credibility of these models and to guide model improvements. In this study the Goddard Chemistry, Aerosol, Radiation, and Transport (GOCART) module running on-line inside the Goddard Earth Observing System version 5 (GEOS-5) model is used to simulate aerosol and SO₂ concentrations. Data taken in November 2010 over Frostburg, Maryland during an SO₂ field campaign involving ground instrumentation and aircraft are used to evaluate GEOS-5 simulated SO₂ concentrations. Preliminary data analysis indicated the model overestimated surface SO₂ concentration, which motivated the examination of mixing processes in the model and the specification of SO₂ anthropogenic emission rates. As a result of this analysis, a revision of anthropogenic emission inventories in GEOS-5 was implemented, and the vertical placement of SO₂ sources was updated. Results show that these revisions improve the model agreement with observations locally and in regions outside the area of this field campaign. In particular, we use the ground-based measurements collected by the United States Environmental Protection Agency (US EPA) for the year 2010 to evaluate the revised model simulations over North America.

1 Introduction

Sulfur dioxide (SO₂) is a trace gas which poses significant health threats near the surface, with consequences on human health (Ware et al., 1986; US EPA, 2011) and on the ecosystem acidification (Schwartz, 1989). With a mean lifetime of few days in the troposphere (Lee et al., 2011; He et al., 2012), emitted SO₂ is quickly oxidized to form sulfate aerosols. The resulting aerosols exert influences on the atmospheric radiative balance and cloud microphysics (e.g., McFiggans et al., 2006). SO₂ is emitted into the atmosphere mainly from anthropogenic sources such as fossil fuel combustion and industrial facilities. In the US these emissions represent more than 90% of SO₂ released into the air (US EPA, 2011). Since the implementation of national environmental regulations (e.g. 1990 Clean Air Act Amendments in the United States), a significant decrease of these emissions has been observed over the past 30 years. To keep track of SO₂ emissions, this gas is monitored throughout the country by a system of continuously sampling ground-based instruments, and also by episodic intensive field campaigns. These campaigns are particularly valuable because the instruments deployed on the ground and from aircraft give not only the opportunity to validate and improve the ability of space-based instruments to monitor air pollutants, but also provide the opportunity to evaluate chemical transport models that simulate the SO₂ and sulfate lifecycle (Easter et al., 2004; Liu et al., 2005; Goto et al., 2011). The purpose of this paper is to take advantage of the data measured during the Frostburg field campaign held in Maryland during November 2010 to evaluate the SO₂ simulated with the GEOS-5/GOCART model. We first describe in Section 2 the aerosol model and give a brief description of the SO₂ sources and the chemical processes considered within the model. In Section 3 we start by validating the modeled SO₂ at the surface over the continental US using the data collected by EPA. In Section 4 we evaluate the GEOS-5 simulated SO₂ with measurement

Correspondence to: Virginie Buchard
(virginie.j.buchard-marchant@nasa.gov)

data taken during the campaign. Section 5 reports the conclusions.

2 Representation of Aerosols in the GEOS-5 Earth Modeling System

The Goddard Earth Observing System version 5 (GEOS-5) model, the latest version from the NASA Global Modeling and Assimilation Office (GMAO), is a weather and climate capable model described by Rienecker *et al.* (2008). The GEOS-5 system includes atmospheric circulation and composition, oceanic and land components. By including an aerosol transport module based on the Goddard Chemistry Aerosol Radiation and Transport (GOCART) model (Chin *et al.*, 2002), GEOS-5 provides the capability of studying atmospheric composition and aerosol-chemistry-climate interaction (Colarco *et al.*, 2010). In addition to providing reanalyses of traditional meteorological parameters (winds, pressure and temperature fields, Rienecker *et al.* (2008)), the inclusion of aerosols provides the background information for GEOS-5 to produce reanalyses of aerosol fields using retrieved aerosol optical depth (AOD) from the space-based instrument Moderate Resolution Imaging Spectroradiometer (MODIS). The GEOS-5 near-real time system runs at a nominal 25 km horizontal resolution with 72 vertical levels between the surface and about 80 km. For this study, the model was run at various horizontal resolutions, $0.25^\circ \times 0.315^\circ$ with sensitivity experiments also carried out at $0.5^\circ \times 0.625^\circ$ latitude by longitude.

GEOS-5 can be run in climate simulation, data assimilation, or replay modes. In the data assimilation mode, a meteorological analysis is performed every six hours to constrain the meteorological state of the model. In the replay mode, a previous analysis, generated with the same version of model, is used to adjust the model's meteorological state much like a Chemical Transport Model (CTM) with the difference that in GEOS-5 the aerosol transport dynamics are entirely consistent with the model thermodynamical state at every time step between analysis updates. For our replay simulations the GMAO atmospheric analyses from the Modern Era Retrospective analysis for Research and Applications (MERRA) (Rienecker *et al.*, 2011) available every six hours are used.

The GOCART module simulates five aerosol types: dust, sea salt, black carbon, organic carbon and sulfate aerosol. The sulfur chemistry processes considered are based on Chin *et al.* (2000a). Sulfate aerosol is mostly formed from the oxidation of SO₂. All simulations include emissions of dimethylsulfide (DMS), SO₂ and sulfate and we use prescribed oxidant fields (hydroxyl radical (OH), nitrate radical (NO₃) and hydrogen peroxide (H₂O₂)) from a monthly varying climatology produced from simulations in the NASA Global Modeling Initiative (GMI) model (Duncan *et al.*, 2007; Strahan and Douglas, 2004). A small amount of SO₂ is produced by the oxidation of DMS, which is emitted naturally from marine phytoplankton. We use a monthly vary-

SO₂ emissions from coal fired plants in 2007



Fig. 1. SO₂ emissions released by coal fired plants in 2007 over the United States (EPA source available at <http://www.epa.gov/cleanenergy/energy-resources/egrid/>). The circle size is proportional to the emission rates.

ing climatology of oceanic DMS concentrations (Kettle *et al.*, 1999), with emissions calculated using the surface wind-speed dependent (Liss and Merlivat, 1986) parameterizations of air-ocean exchange processes. The main source of SO₂ is anthropogenic, mainly from fossil fuel combustion from power plants and industrial activities (US EPA, 2011).

Figure 1 maps the emissions of SO₂ released from coal fired power plants (in tons) over the US in 2007. In this study, two different data sets of anthropogenic emissions and two assumptions about the injection height are considered in our simulations to assess the effect of the emissions on SO₂ surface concentration. At the time of the campaign, the annual anthropogenic emissions of SO₂ were taken from Streets *et al.* (2009). In the GEOS-5 control simulation, this emission was injected into the lowest model level. All simulated results using this configuration are hereafter called the "Control Run" or CR.

Recently, a new Emission Database for Global Atmospheric Research (EDGAR) version v4.1 dataset (European Commission, 2010) became available at 0.5° horizontal resolution and has the advantage of providing the 2005 anthropogenic emissions of SO₂ by source categories. This new set of emissions allowed us to emit the non-energy emissions (from transportation, manufacturing industries, residential) into the lowest GEOS-5 layer and the energy emissions from power plants at higher levels between 100 and 500 meters (between the 2nd and 4th model layers). The results are herein referred to as the "Revised Run" or RR.

Figure 2 shows a comparison of the SO₂ anthropogenic emissions by source category: energy-source sector and non-energy-source sector, based on the EDGAR 2005 database as used in our revised simulation. Most SO₂ emissions are released from power plants, so it is important to consider the emission injection above 100 m due to the stack height and

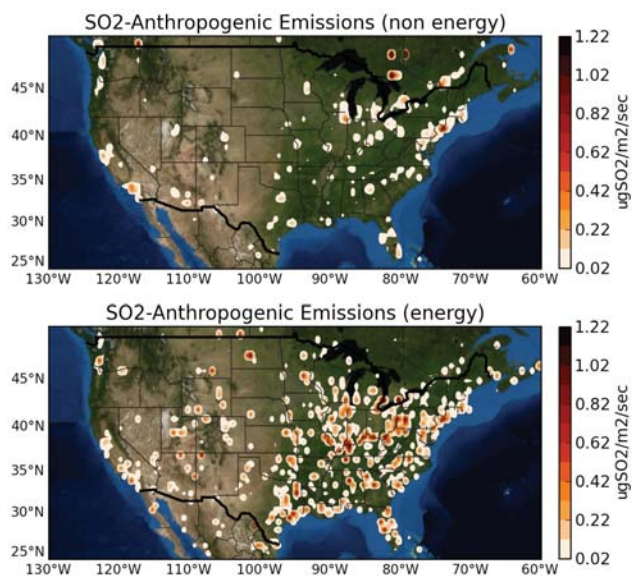


Fig. 2. SO₂ anthropogenic emissions from the EDGAR v4.1 regrided at 0.25°x0.3125° resolution in 2005 for non energy and energy sectors.

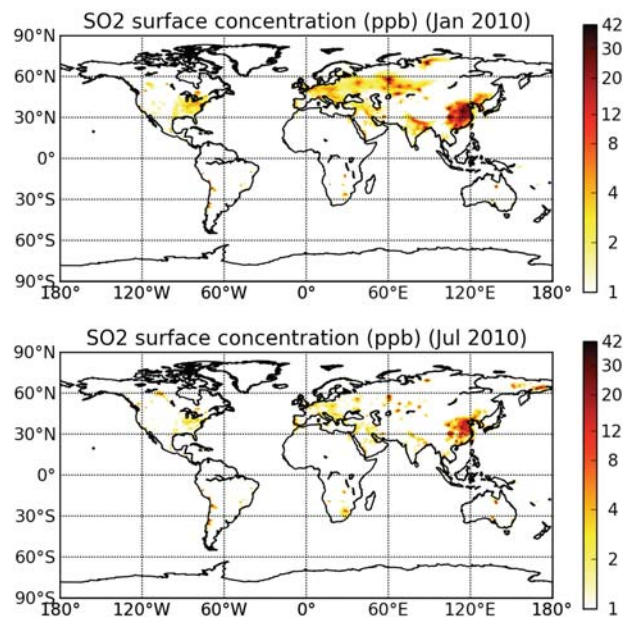


Fig. 3. GEOS-5/GOCART monthly mean of SO₂ surface-level (revised run) for January and July 2010.

155 plume rise. We assume these emissions are constant throughout the year. Furthermore, other anthropogenic emissions include aircraft and ship traffic emissions from Mortlock et al. (1998) and Eyring et al. (2005) respectively. We assume 3% of the SO₂ anthropogenic emissions are directly emitted as sulfate. All the simulations include also biomass burning emissions of SO₂ following the Quick Fire Emission Dataset (QFED) inventory and SO₂ emissions from continuously eruptive volcanoes that are based on data from the Global Volcanism Program database (Siebert et al., 2002) and Total Ozone Mapping Spectrometer (TOMS) and Ozone Monitoring Instrument (OMI)'s SO₂ retrievals (Carn et al., 2003; Krotkov et al., 2006) while emissions from explosive volcanoes follow the AeroCom inventories (Dentener et al., 2006). SO₂ is removed in the atmosphere by dry and wet deposition and oxidized to sulfate by chemical reaction. The main oxidation pathways are in the aqueous phase by H₂O₂ and in the gas phase by OH (Chin et al., 2000a). We save the model tracer fields every three hours during our simulation. Figure 3 shows results of the simulated SO₂ surface concentrations for January and July 2010. The highest SO₂ concentrations are found over eastern Asia, Europe, and North America, which are major anthropogenic source regions. SO₂ concentrations are higher during the winter; this seasonal variation can be explained by the seasonal SO₂ oxidation rates, which are slower in winter than in the summer (Chin et al., 2000b). The planetary boundary layer (PBL) dynamics is also responsible for this seasonal cycle of SO₂ concentrations. Figure 4 shows an evaluation of the GEOS-5 simulation of the SO₂ lifetime in black by comparison with the analysis made by Lee et

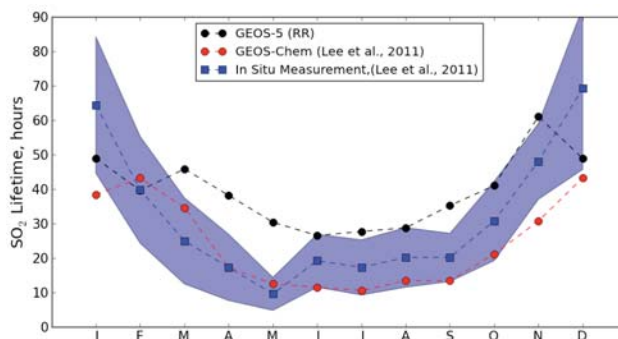


Fig. 4. GEOS-5/GOCART monthly SO₂ lifetime for the year 2010 compared to the study made by Lee et al. (2011) over the eastern United States (35.2°N - 44.5°N, 68.4°W - 81.6°W) during daytime.

al. (2011) with the GEOS-Chem chemical transport model in red and in-situ measurements-based lifetime in blue. The mean SO₂ lifetime from GEOS-5 simulations are calculated over the eastern US (35.2°N - 44.5°N, 68.4°W - 81.6°W) and during daytime as Lee et al. (2011) but for the year 2010. The seasonal variation of the SO₂ lifetime from GEOS-5 is globally consistent with the seasonal variation found with the GEOS-chem model and the in-situ measurements. While the mean SO₂ lifetime from GEOS-chem are generally shorter than the in-situ measurement-based lifetime, the mean SO₂ lifetime from GEOS-5 simulations are generally higher than the in-situ measurements, except during the winter. However,

the GEOS-5 SO₂ lifetime values are quite close or within the range defined by the uncertainty interval of in-situ measurements. The differences in the transport and in the emissions are among the possible reasons that may explain the discrepancy with the GEOS-Chem model. In addition the oxidant fields in GEOS-5 are not interactive and depend instead on fields from a different model from a different period.

3 Model comparison to EPA surface measurements

In this section we evaluate the modeled surface concentrations of SO₂ and sulfate over the US for the control and revised runs for the year 2010. For this study we used data collected by EPA, local and state control agencies which maintain air quality monitoring networks over the US available from the EPA Air Quality System (AQS) (US EPA, 2010).

3.1 Sulfur dioxide

Figure 5 shows the SO₂ daily mean comparisons for the control run (top) and the revised run (middle). The "EPA" daily averages of SO₂ concentration were calculated using hourly concentrations collected from 102 sites obtained from the EPA AQS. A kernel density estimation (KDE) (Silverman, 1986; Scott, 1992) was applied to approximate the joint probability density function (PDF) of observed and modeled SO₂ daily mean surface concentrations. Since SO₂ is usually log-normally distributed, the correlation coefficient (r), the Root Mean Square of the differences (GEOS-5-EPA) (RMS), the standard deviation (STDV) and the mean differences are calculated for logarithmically transformed data (summarized in Table 1 as well as the parameters in the original units calculated using the equations described in Limpert *et al.* (2001) (Appendix A)). For both plots, the scatter between modeled and observed daily means is significant with correlation coefficients, $r=0.49$ and $r=0.42$ for the control and revised run respectively. However, the agreement between the observed and modeled daily mean is better with the revised run, with lower values for the RMS and the mean difference. The STDV is almost the same for both the control and revised runs. One of the reasons for this discrepancy might be attributed to the change in absolute magnitude of the SO₂ emissions datasets used in the control and revised runs, but we noticed only small differences between the two datasets. Another plausible explanation is the emission injection height considered in the model. The vertical placement of emissions in the revised run decreases the high bias between observations and simulations at the surface. The remaining bias between observations and revised model SO₂ simulations may be explained by the error of representativeness associated with the incompatibility between in-situ measurements and grid-box mean values predicted by the model. As an attempt to filter out the in-situ measurements that are very unrepresentative of the grid-box mean

conditions, the bottom plot of Fig. 5 presents the results after a statistical quality control was performed with the adaptive buddy check of Dee *et al.* (2001). For a given ob-

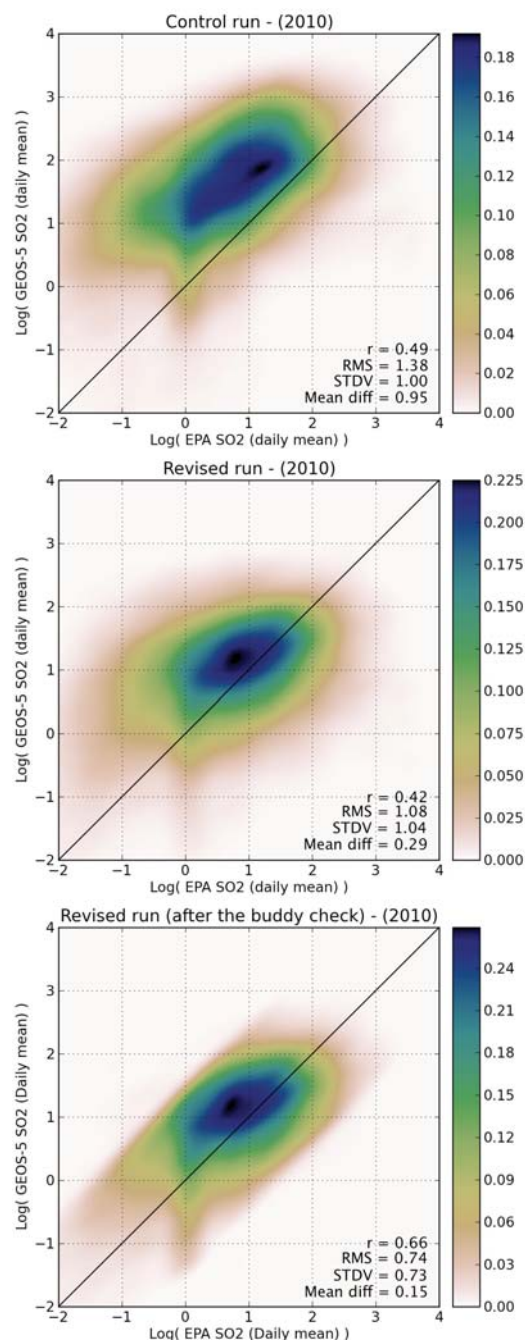


Fig. 5. Comparison of daily averaged surface SO₂ concentration in 2010 for 102 EPA sites. The model results are from the control run (top), the revised run (middle) and after the adaptive buddy check of Dee *et al.* (2001) was performed on the model revised simulations (bottom) (RR/bc).

servation, this method consists of looking at nearby model-

Table 1. Summary of SO₂ surface comparison results (n is the number of points; r is the correlation coefficient; STDV is the standard deviation and \overline{diff} is the mean difference in the logarithmic scale, the parameters with a '*' are the values in the original data scale as described in Limpert *et al.* (2001), Appendix B).

	n	r (log)	STDV (log)	STDV* (ppb)	RMS (log)	RMS* (ppb)	\overline{diff} (log)	\overline{diff}^* (ppb)
Control run	24916	0.49	1.00	5.64	1.38	7.08	0.95	4.29
Revised run	27435	0.42	1.04	3.22	1.08	3.95	0.29	2.29
Revised run/buddy-check	22538	0.66	0.73	1.27	0.74	1.98	0.15	1.52

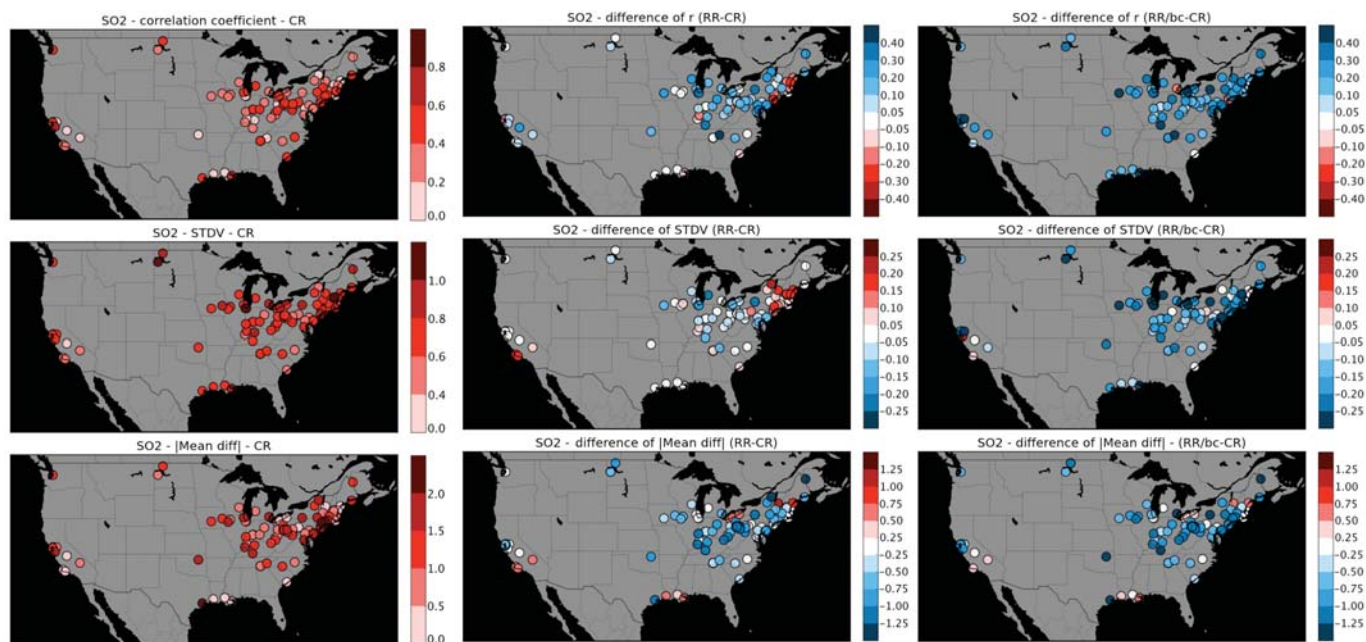


Fig. 6. The first column is r, the STDV and the absolute value of the mean difference between the modeled (control run) and observed daily averaged SO₂ surface concentrations for each SO₂ EPA site in 2010. The second column is the change in r, STDV, and absolute value of the mean difference for the revised run relative to the control run. The third column is the same, but showing the difference between the revised run (with buddy check of Dee *et al.* (2001)) and the control run. The color coding in the second and third column is such that blue indicates improvement relative to the control run.

observations discrepancies and discarding those observations that cannot be corroborated by their neighbors. A brief summary of the algorithm is given in Appendix B. After removing observations that failed this adaptive buddy check (Fig. 5 - bottom plot), the new comparison is quite improved with r that increased and is equal to 0.66 and lower values of the RMS, SDTV and the mean difference. The explanation for the remaining bias observed after the quality control could be the year (2005) of the emission dataset with emissions too high for the year 2010. According to EPA (e.g., <http://www.epa.gov/air/airtrends/sulfur.html>) the average SO₂ concentrations have decreased substantially over the years because of the application of SO₂ control measures. Based on 341 US monitor sites, a 60% decrease in national average was found between 2000 and 2010. If we

look site by site, Fig. 6 presents the change in the r (top), the STDV (middle) and the absolute value of the mean difference (bottom) between modeled and observed daily averaged surface SO₂ for the control run on the left, the revised run in the middle and after the buddy check on the right. While the correlation coefficient increased from values lower than 0.4-0.6 for the control run to values greater than 0.6 after the buddy check, we see that the STDV increased over New England and slightly decreased elsewhere for the revised run, the decrease is more significant after the buddy check. Concerning the absolute value of mean difference, we notice a decrease more and more significant between the control, the revised run and after the buddy-check.

3.2 Sulfate aerosol

Figure 7 shows comparisons similar to the ones on Fig. 5, but for sulfate. The daily means are directly provided by the EPA AQS and are available every one, three or six days for a total of 250 sites. Figure 7 includes also a comparison with the sulfate simulated with the GEOS-5 aerosol assimilation system, assimilation of MODIS AOD in the revised version of the model has been performed. On average the modeled sulfate concentrations are higher than the observations, regardless of the model or data assimilation system used. The values of r , the RMS, STDV and the average differences are slightly different for the control, revised simulations and the reanalysis (summarized in Table 2). This suggests that the SO₂ emissions injections as well as the assimilation of AOD observations into the model have a low impact on the daily mean sulfate comparisons. Like for the SO₂ study, the measurements have been quality controlled using the buddy-check scheme (Fig. 7), permitting an increase r from 0.71 to 0.79, the RMS, the STDV and the mean difference have been divided by almost a factor 2. Coupled with the longer lifetime of SO₂ in Fig. 4 and 5 and, hence, too slow production of sulfate, our results suggest we may strongly underestimate the losses of sulfate aerosol. When looking site by site (Fig. 8), while the values of r decrease with the revised simulations for some sites, the application of the buddy check lead generally to greater and significant correlation coefficient values; the STDV values have not really changed between the control and revised runs but the values tend to decrease after the buddy check. Finally we see also an improvement in the absolute values of the mean differences after the revised and more importantly after the buddy check simulations.

4 Evaluation of SO₂ in the model: comparison with measurement data during the Frostburg campaign in Maryland

In Section 4 we concentrate our evaluation of the model performance in a smaller region using data collected during an air quality campaign in western Maryland in November 2010. The Frostburg campaign was a regional air quality campaign conducted by investigators from Washington State University (WSU), the University of Maryland (UMD) and the NASA Goddard Space Flight Center (GSFC) during two weeks in November 2010. The campaign took place in Western Maryland and provided direct measurements of SO₂ among other atmospheric constituents. The interest of this region is based on the abundance of SO₂ from the Ohio River Valley, surrounded by several power plants (Figure 9). In this section, we make use of several data sets available during this campaign to evaluate the anthropogenic SO₂ concentration simulated by GEOS-5.

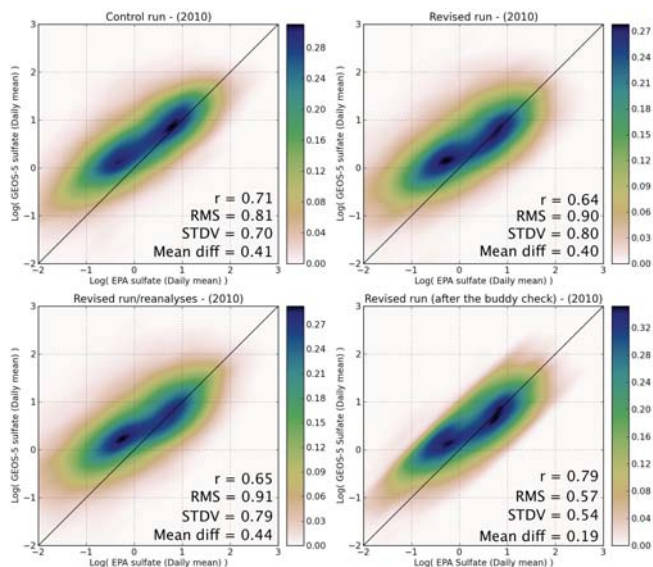


Fig. 7. Comparison of daily averaged sulfate surface concentrations for 250 EPA sites in 2010. The model results are from the control run, the revised run, the aerosol assimilation system and the revised simulations combined with the buddy check of Dee *et al.* (2001).

4.1 Surface analysis: comparisons at Piney Run Station

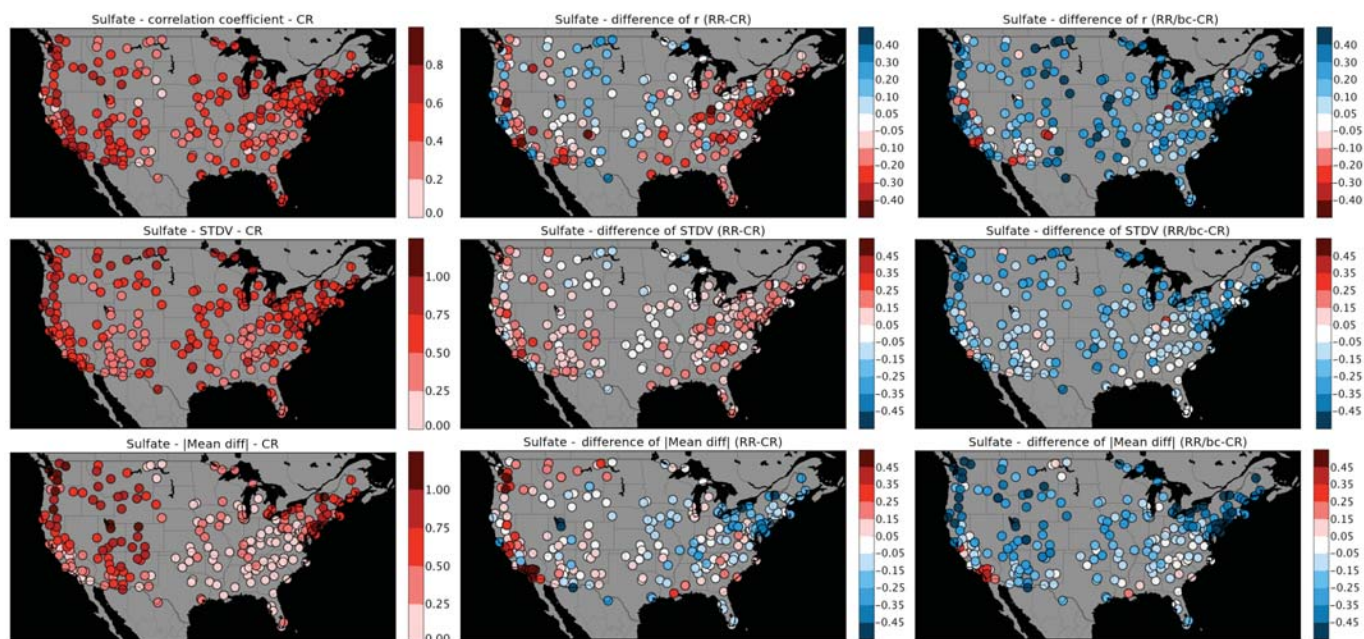
The observed and simulated monthly mean SO₂ at the surface at Piney Run station are shown in Figure 10. This site is located in a mountain valley close to Frostburg, and is an ideal location for SO₂ monitoring due to its close proximity to power plants stations, with the nearest one, Warrior Run, located south of Cumberland. Globally, the model captures the observed month-to-month variability of SO₂ with a winter maximum for both the control run in red and the revised run in black, as stated in section 2, the oxidation rates and the PBL dynamics are responsible for this seasonal variation.

In the control run (the red line in Figure 10), we see that the model overestimates the observed SO₂ values by a factor of 4-5. This result is consistent with the general findings of section 3: the revised vertical placement of SO₂ emissions has a positive impact on the simulated surface values of SO₂. This is shown with the revised run (in black) where the model values are in better agreement with the observations and the overestimation is less than a factor 2. Like seen previously, an explanation of the positive bias remaining might be attributed to the 2005 emissions inventory and the recent decreasing trend of SO₂ pollution over the US noted by EPA. In particular in Piney Run, the concentrations of SO₂ decreased 50% between 2006 and 2010.

Figure 11 shows the comparison of the daily mean SO₂ surface concentrations to the measurements at Piney Run during 2010. Again, we see the better agreement between the revised run and the observations.

Table 2. Summary of sulfate comparison results.

	n	r (log)	STDV (log)	STDV* ($\mu\text{g}/\text{m}^3$)	RMS (log)	RMS* ($\mu\text{g}/\text{m}^3$)	\overline{diff} (log)	\overline{diff}^* ($\mu\text{g}/\text{m}^3$)
Control run	17707	0.71	0.70	1.54	0.81	2.46	0.41	1.92
Revised run	19658	0.64	0.80	1.95	0.90	2.84	0.40	2.06
Revised run / aerosol reanalyses	19657	0.65	0.79	1.99	0.91	2.92	0.44	2.12
Revised run / buddy-check	16444	0.79	0.54	0.81	0.57	1.62	0.19	1.40

**Fig. 8.** Same as figure 5 but for daily averaged sulfate surface concentrations.

5 Column amount analysis: comparisons to a MF-DOAS instrument

Simulated SO₂ column amount is evaluated with measurements from the Multifunction Differential Optical Absorption Spectroscopy (MFDOAS) instrument developed at WSU (Herman *et al.*, 2009; Spinei *et al.*, 2010), deployed on the roof of a building at Frostburg State University (FSU) for the campaign. This instrument measures the direct sun irradiance and scattered sunlight in spectral UV and visible wavelengths 281 - 498 nm at 0.83 nm spectral resolution recorded simultaneously with a CCD detector in the spectrograph focal plane. Analysis of the measured spectra is done using the DOAS technique which is based on the Beer-Lambert law which states that the relationship at a wavelength between the intensity of the incident solar light and the transmitted one attenuated due to absorption and scattering by aerosols and molecules in the atmosphere (e.g., Platt, 1994; Plane and Smith, 1995). SO₂ column density is measured with an un-

certainty less than 0.03 DU. A description of this instrument as well as the DOAS technique can be found in Spinei *et al.* (2010). Figure 12 shows the comparison between the column density measured by the MFDOAS and simulated by GEOS-5 during daylight hours from 13:30 UTC until 21:00 UTC on November 08 and 09. We notice that changing from one emission dataset to the other shows not much change on the total column amount between the two runs; it confirms the small changes in the absolute magnitude of the SO₂ emissions between the two datasets. Accounting for the uncertainty on the ground-based instrument, the comparison is rather satisfying with both the control and revised run but we notice that the model does not reproduce the observed diurnal variations. Besides the lack of diurnal variation in the prescribed emissions, an explanation might be the spatial resolution of the model (~ 25 km) and the offset pointing of the MFDOAS instrument when looking at the sun.

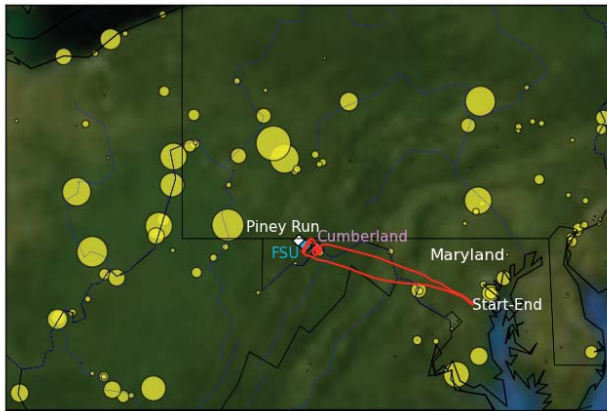


Fig. 9. Frostburg campaign regional map. Yellow circles are coal fired power plant stations; the circle size is proportional to the emission rates. Piney Run station denoted by the white symbol \diamond is located at 39.70°N and -79.01°W . Cumberland (in pink) is located at 39.62°N and -78.77°W and the Frostburg State University (in blue) is located at 39.65°N and -78.93°W . Flight track on 11/08/2010 is in red.

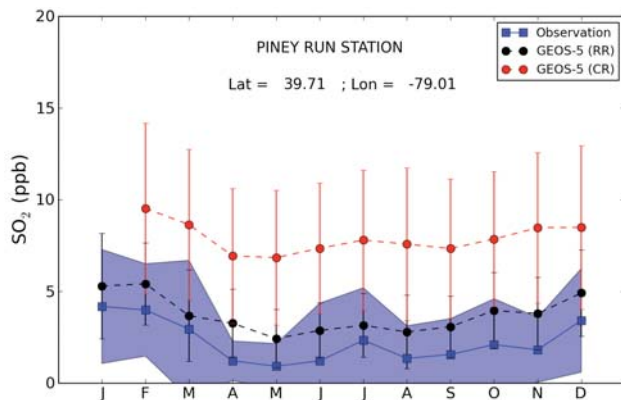


Fig. 10. Monthly averaged concentrations of SO₂ at the surface in 2010 at the Piney Run station. Blue squares are observations, red circles are model simulations with the control run, black circles are revised model simulations. Vertical bars are the standard deviations of monthly values for the model, shaded blue area for observations.

5.1 Vertical analysis: comparisons to aircraft measurements

The GEOS-5 simulated vertical distribution of SO₂ is compared to aircraft measurements conducted on two different days during the campaign. The flights were made on the UMD Cessna 402B aircraft, which was equipped with a modified pulse-fluorescence instrument to measure the in situ SO₂ concentration (Taubman *et al.*, 2006). The aircraft flight path on November 8 is shown on Fig. 9. Important regional power plants are marked by yellow circles in Figure 9, with

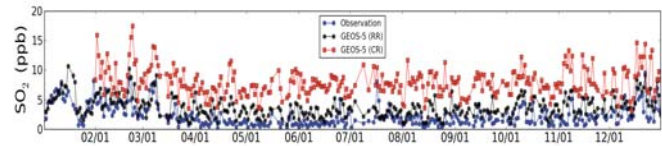


Fig. 11. Times series of daily averaged concentrations of SO₂ at the surface in 2010 at Piney Run station. Blue squares are observations, red circles are model simulations with the control run, black circles are revised model simulations.

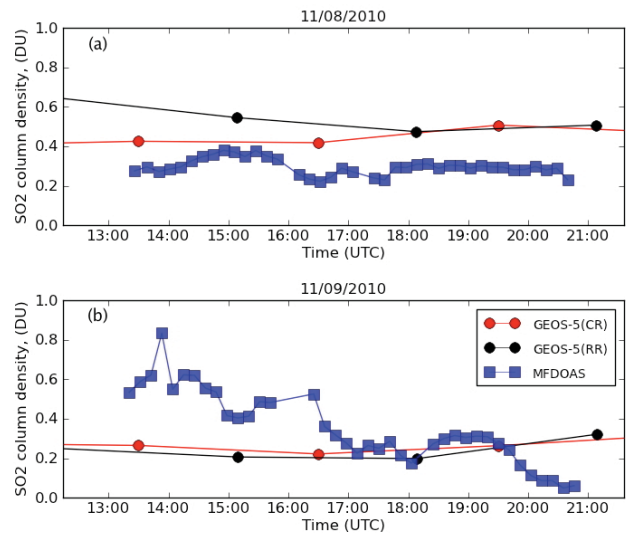


Fig. 12. Daily variations of the SO₂ total column amount on 11/08/2010 (top) and 11/09/2010 (bottom) at the Piney Run Station. Blue squares are MFDOAS measurements, red and black circles are model simulations with the control and revised runs respectively.

the size of the circle indicating the magnitude of SO₂ emissions. November 8, 2010 featured sustained winds as high as 29 km/h with gusts to 45 km/h around the time of the flight. November 9, 2010 was considerably calmer, with sustained winds under 19 km/h and gusts noted over Cumberland around the time of the flight. These information were recorded at the airport, which is not an official National Weather Service reporting station, but they were also backed up by the informal observations of the airplane's crew. Both flights lasted about two hours and were characterized by spiraling climbs and descents over Frostburg (39.65°N , -78.93°W) and Cumberland, Maryland (39.62°N , -78.77°W). Figure 13 shows the simulated vertical profile of SO₂ for the control (left) and revised (middle) runs sampled along the aircraft flight path, as well as the comparisons of the modeled SO₂ concentration from the revised run only to the aircraft observations for both days. The dark black lines in Figure 13 show the modeled SO₂ extracted exactly at the aircraft

420 position, while the blue shading shows the range of the modeled SO₂ concentrations for the surrounded grid boxes (25 km in the horizontal direction and 200 meters in the vertical direction). If we look at the vertical profiles comparisons between the control and revised runs, we notice small changes
 425 between the two runs. On November 8th, GEOS-5 captures most of the major features of the aircraft observations, including the sharp vertical gradient encountered as the aircraft made its vertical profile near Cumberland (at about 60 minutes of flight time). The turbulent mixing and strong winds during this day explain the air well mixed and coming from a much larger area. On November 9th the model also captures many of the aircraft variations but misses the observed high values between 60-80 minutes flight time. During this time frame, the aircraft was flying over Cumberland, near the coal
 430 fired power plant Warrior Run. The calmer weather conditions during this day may explain the high values observed locally that could not be reproduced by the model with a 25 km resolution. Concerning the simulated surface-level SO₂, like seen in more details in sections 3.1 and 4.1 we notice a slight overestimation of the SO₂ surface-level concentration at the beginning and at the end of the flight on both days. 485

6 Conclusions

The Frostburg campaign that took place in Maryland in November 2010 was a good opportunity to evaluate the SO₂ simulated by the GEOS-5/GOCART system. By comparing the modeled SO₂ against observed data, such as aircraft and ground-based measurements from a ground-based system in Frostburg, we have first diagnosed that the SO₂ concentrations was overestimated at the surface and adjusting the vertical placement of the SO₂ anthropogenic emissions inside
 445 GEOS-5 improved the SO₂ surface concentrations without changing considerably the integrated total column amount. The improvement in our treatment of the SO₂ anthropogenic emissions was confirmed with the analysis performed over the US using the EPA ground-based measurements. 500

The comparisons of the vertical profile with aircraft data showed that despite the spatial coarse resolution of GEOS-5, most of the major features of the aircraft observations were reproduced by the model on November 8 because the weather
 450 was dynamic with turbulent mixing and strong winds. In contrast the analysis on November 9 shows that during quiet days, GEOS-5 will have difficulty of detecting plumes, especially in the vicinity of point source. Concerning the GEOS-5 simulated sulfate, the comparisons with the EPA data show that the changes in the SO₂ emissions dataset and vertical distribution did not affect much the simulation of the sulfate at the surface, the positive bias observed with the control run remains with the revised run. These comparisons suggests that there might have an underestimated loss of sulfate in the model. A full analysis of the chemical processes could not
 460 be performed with the available data and there is a possibil-

ity that part of this process could also explain part of the bias remaining in the SO₂ and sulfate comparisons.

Appendix A

The lognormal distribution

A random variable X is lognormally distributed if $Y = \log(X)$ has a normal distribution. The mean \bar{X} and the standard deviation s_X of the normal variable are related to the \bar{Y} and s_Y of the lognormal variable by (Limpert et al., 2001) :

$$\bar{X} = \exp(\bar{Y} + s_Y^2/2) \quad (\text{A1})$$

$$s_X = \bar{X} \sqrt{\exp(s_Y^2 - 1)} \quad (\text{A2})$$

Appendix B

Adaptive Buddy Check

In the buddy-check algorithm of Dee et al. (2001), first a background check is performed where differences between the observed and modeled daily means are analyzed in order to identify a set of suspect observations, given a specified tolerance. An iterative buddy-check is then performed on each suspect observation using the remaining reliable observations (called "buddies") within a specified radius to perform a refined acceptance test. The tolerance used for this buddy check is adaptive in the sense that current values of the observation minus model departures are used as a local modulator of the innovation variances used in the threshold test. Notice that before applying the buddy check the observation-model departures must be unbiased by removing the mean value. Figure B1 shows the PDF of the points removed after the buddy check is performed for SO₂. Although in some cases GEOS-5 simulates lower SO₂ surface values than the ground-based measurements, the majority of points removed after the buddy check are due of an overestimation of the GEOS-5 simulations compared to EPA measurements. While misplacement of plumes by the model could account for some large discrepancies that would be flagged by the buddy check, there is no reason to expect that these discrepancies would be of a given sign. Therefore, the positive bias of the removed observations may point to excessive emissions by GEOS-5 at specific locations.

Acknowledgements. The campaign participants want to acknowledge significant logistical support from Dr. J. Hoffman (dean of Sciences) and the operations staff at Frostburg State University. WSU acknowledges NASA grant NNX09AJ28G for instrument development and deployment. The authors would like to thank Lacey Brent, flight scientist, for collecting the aircraft data.

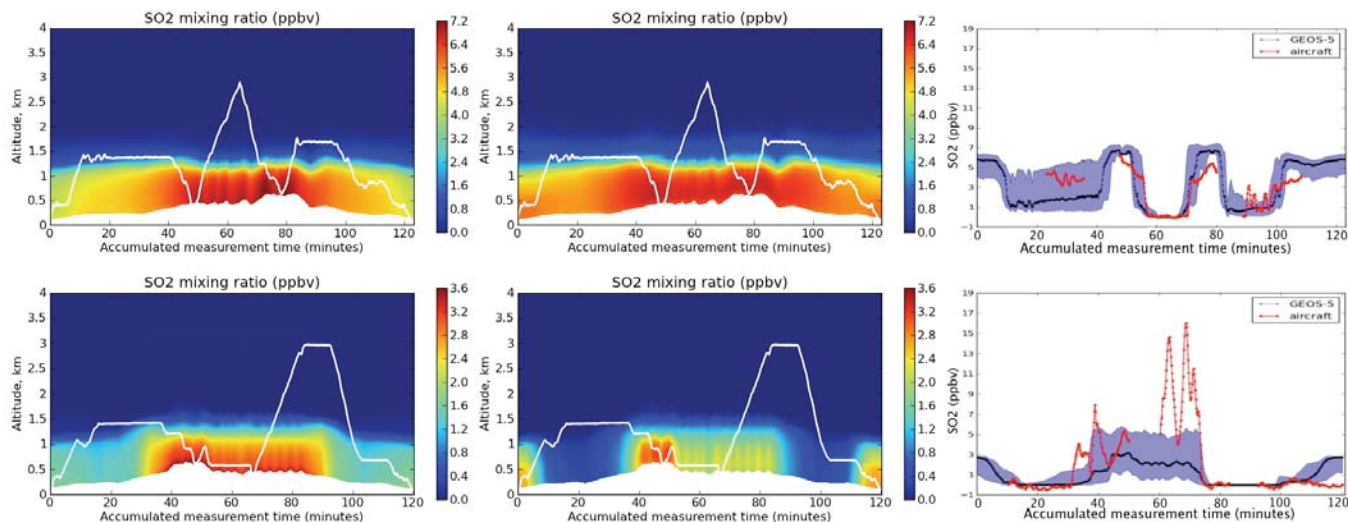


Fig. 13. GEOS-5/GOCART SO₂ simulations for the control run (left), the revised run (middle) along the flight track on 11/08/2010 (top), on 11/09/2010 (bottom). Modeled SO₂ vertical profiles for the control run (left) and revised run (middle), the white line is the aircraft altitude, on the right, the red line is the observed SO₂ concentration, the black line is the modeled SO₂ concentration (revised run), and the blue shading shows the range of simulated SO₂ for the surrounded grids.

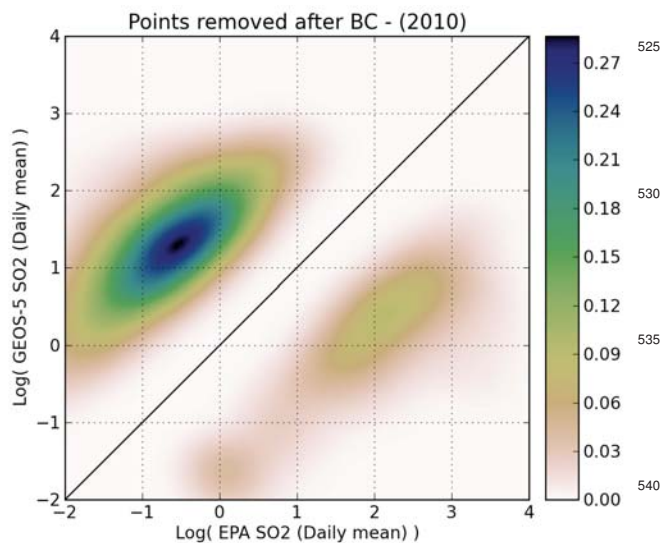


Fig. B1. Points removed after the adaptive buddy check of Dee *et al.*, (2001) was performed on the model revised SO₂ simulations.

References

Bey, I., Jacob, D. J., Yantosca, R. M., Logan, J. A., Field, B. D., Fiore, A. M., Li, Q. B., Lui, H. G. Y., Mickley, L. J., and Schultz, M. G.: Global modeling of tropospheric chemistry with assimilated meteorology: Model description and evaluation, *J. Geophys. Res.*, 106(D19), 2307323095, 2001.

Carn, S. A., Krueger, A. J., Bluth, G. J. S., Schaefer, S. J., Krotkov,

N. A., Watson, I. M., and Datta, S.: Volcanic eruption detection by the Ozone Mapping Spectrometer (TOMS) instruments: a 22-year record of sulphur dioxide and ash emissions, in: *Volcanic Degassing, Special Publication of the Geological Society of London No. 213*, edited by: Oppenheimer, C., Pyle, D. M., and Barclay, J., Geological Society, London, UK, 177202, 2003.

Chin, M., Rood, R. B., Lin, S.-J., Miller, J.-F. and Thompson, A. M.: Atmospheric sulfur cycle simulated in the global model GOCART: Model description and global properties, *J. Geophys. Res.*, 105(D20), 24,67124,687, doi:10.1029/2000JD900384, 2000a.

Chin, M., Savoie, D. L., Huebert, B. J., Bandy, A. R., Thornton, D. C., Bates, T. S., Quinn, P. K., Saltzman, E. S., and De Bruyn, W. J.: Atmospheric sulfur cycle simulated in the global model GOCART: Comparison with field observations and regional budgets, *J. Geophys. Res.*, 105, 2468924712, 2000b.

Chin, M., Ginoux, P., Kinne, S., Torres, O., Holben, B. N., Duncan, B. N., Martin, R. V., Logan, J. A., Higurashi, A., and Nakajima, T.: Tropospheric aerosol optical thickness from the GOCART model and comparisons with satellite and sun photometer measurements, *J. Atmos. Sci.*, 59(3), 461483, 2002.

Colarco, P. R., da Silva, A., Chin, M., and Diehl, T.: Online simulations of global aerosol distributions in the NASA GEOS-4 model and comparisons to satellite and ground-based aerosol optical depth, *J. Geophys. Res.*, 115, D14207, doi:10.1029/2009JD012820, 2010.

Dee, D., Rukhovets, L., Todling, R., da Silva, A. and Larson J.: An adaptive buddy check for observational quality control, *Q. J. R. Meteorol. Soc.*, 127, pp 2451-2471, 2001.

Dentener, F., Kinne, S., Bond, T., Boucher, O., Cofala, J., Generoso, S., Ginoux, P., Gong, S., Hoelzemann, J. J., Ito, A., Marelli, L., Penner, J. E., Putaud, J.-P., Textor, C., Schulz, M., van der Werf, G. R., and Wilson, J.: Emissions of primary aerosol and pre-

- cursor gases in the years 2000 and 1750 prescribed data-sets for AeroCom, *Atmos. Chem. Phys.*, 6, 4321–4344, doi:10.5194/acp-6-4321-2006, 2006.
- 560 Duncan, B.N., Strahan, S.E., Yoshida, Y., Steenrod, S.D. and Livesey, N.: Model study of the cross-tropopause transport of biomass burning pollution. *Atmos. Chem. Phys.*, 7, 3713–3736, 2007.
- Easter, R. C., Ghan, S. J., Zhang, Y., Saylor, R. D., Chapman, E. G., Laulainen, N. S., Abdul-Razzak, H., Lenug, L. R., Bian, X., and Zaveri, R. A.: MIRAGE: Model description and evaluation of aerosols and trace gases, *J. Geophys. Res.*, 109, D20210, doi:10.1029/2004JD004571, 2004.
- 570 European Commission: Joint Research Centre (JRC)/Netherlands Environmental Assessment Agency (PBL): Emission Database for Global Atmospheric Research (EDGAR), release version 4.1., available at: <http://edgar.jrc.ec.europa.eu>, 2010.
- Eyring, V., Kohler, H. W., van Aardenne, J., and Lauer, A.: Emissions from international shipping: 1. the last 50 years, *J. Geophys. Res.*, 110, D17305, doi:10.1029/2004JD005619, 2005.
- 575 Goto, D., Nakajima, T., Takemura, T. and Sudo, K.: A study of uncertainties in the sulfate distribution and its radiative forcing associated with sulfur chemistry in a global aerosol model. *Atmos. Chem. Phys.*, 11, 1088910910, 2011.
- 580 He, H., Li, C., Loughner, C. P., Li, Z., Krotkov, N. A., Yang, K., Wang, L., Zheng, Y., Bao, X., Zhao, G., and Dickerson, R.R.: SO₂ over central China: Measurements, numerical simulations and the tropospheric sulfur budget, *J. Geophys. Res.*, 117, D00K37, 2012.
- 585 Herman, J., Cede, A., Spinei, E., Mount, G., Abushassan, N.: NO₂ Column Amounts from Ground-based Pandora and MF-DOAS Spectrometers using the Direct-Sun DOAS Technique: Intercomparisons and Application to OMI Validation. *J. Geophys. Res.*, 114, D13307, 2009.
- 590 Kettle, A. J., Andreae, M. O., Amouroux, D., Andreae, T. W., Bates, T. S., Berresheim, H., Bingemer, H., Boniforti, R., Curran, M. A., DiTullio, G. R., Helas, G., Jones, G. B., Keller, M. D., Kiene, R. P., Leck, C., Levasseur, M., Malin, G., Maspero, M., Matrai, P., McTaggart, A. R., Mihalopoulos, N., Nguyen, B. C., Novo, A., Putaud, J. P., Rapsomanikis, S., Roberts, G., Schebeske, G., Sharma, S., Simo, R., Staubes, R., Turner, S., and Uher, G.: A global database of sea surface dimethylsulfide (DMS) measurements and a procedure to predict sea surface DMS as function of latitude, longitude and month, *Global Biogeochem. Cy.*, 13, 399444, 1999.
- 600 Krotkov, N. A., Carn, S. A., Krueger, A.J., Bhartia, P. K., and Yang, K.: Band residual difference algorithm for retrieval of SO₂ from the Aura Ozone Monitoring Instrument (OMI), *IEEE Trans. Geosci. Remote Sens.*, 44(5), 12591266, doi:10.1109/TGRS.2005.861932, 2006.
- 605 Lee, C., Martin, R. V., van Donkelaar, A., Lee, H., Dickerson, R. R., Hains, J. C., Krotkov, N., Richter, A., Vinnikov, K., and Schwab, J.J.: SO₂ emissions and lifetimes: Estimates from inverse modeling using in situ and global, space-based (SCIAMACHY and OMI) observations, *J. Geophys. Res.*, 116, D06304, doi:10.1029/2010JD014758, 2011.
- 610 Limpert, E., Stahel, W. A. and Abbt, M.: Log-normal Distributions across the Sciences: Keys and Clues, *BioScience*, Vol. 51 No.5, 2001.
- 615 Liss, P. S., and Merlivat, L.: Airsea gas exchange rates: Introduction and synthesis, in *The Role of Air-Sea Exchange in Geochemical Cycling*, edited by P. Buat-Mnard, pp. 113127, Springer, New York, 1986.
- Liu, X. H., Penner, J. E., and Herzog, M.: Global modeling of aerosol dynamics: Model description, evaluation, and interactions between sulfate and nonsulfate aerosols, *J. Geophys. Res.*, 110, D18026, doi:10.1029/2004JD005674, 2005.
- McFiggans, G., Artaxo, P., Baltensperger, U., Coe, H., Facchini, M. C., Feingold, G., Fuzzi, S., Gysel, M., Laaksonen, A., Lohmann, U., Mentel, T. F., Murphy, D. M., O'Dowd, C. D., Snider, J. R., and Weingartner, E.: The effect of physical and chemical aerosol properties on warm cloud droplet activation, *Atmos. Chem. Phys.*, 6, 25932649, doi:10.5194/acp-6-2593-2006, 2006.
- Mortlock, A. and Alstyne, R. V.: Military, Charter, Unreported Domestic Traffic and General Aviation 1976, 1984, 1992, and 2015 Emission Scenarios, Contractor Report 1998-207639, National Aeronautics and Space Administration, Hampton, VA, USA, 120 pp., 1998.
- Plane, J.M.C. and Smith, N.: *Advances in Spectroscopy*, v24., John Wiley and Sons, NY, 1995.
- Platt, U.: *Differential Optical Absorption Spectroscopy (DOAS), in Air Monitoring by Spectroscopic Techniques*, edited by M. W. Sigrist, John Wiley, New York, 1994.
- Rienecker, M., Suarez, M. J., Todling, R., Bacmeister, J., Takacs, L., Liu, H.-C., Gu, W., Sienkiewicz, M., Koster, R. D., Gelaro, R., Stajner, I., and Nielsen, J. E.: The GEOS-5 Data Assimilation System-Documentation of Versions 5.0.1, 5.1.0, and 5.2.0., Technical Report Series on Global Modeling and Data Assimilation, 104606, 27, 2008.
- Rienecker, M., Suarez, M. J., Gelaro, R., Todling, R., Bacmeister, J., Liu, E., Bosilovich, M. G., Schubert, S. D., Takacs, L., Kim, G.-K., Bloom, S., Chen, J., Collins, D., Conaty, A., da Silva, A., Gu, W., Joiner, J., Koster, R. D., Lucchesi, R., Molod, A., Owens, T., Pawson, S., Pegion, P., Redder, C. R., Reichle, R., Robertson, F. R., Ruddick, A. G., Sienkiewicz, M., and Woollen, J.: MERRA - NASA's Modern-Era Retrospective Analysis for Research and Applications, *J. Climate*, 24, 36243648, doi:10.1175/JCLI-D-11-00015.1, 2011.
- Schwartz, S. E., Acid deposition: Unraveling a regional phenomenon, *Science*, 243, 753–763, 1989.
- Scott, D. W.: *Multivariate Density Estimation: Theory, Practice, and Visualization*. Wiley, 1992.
- Siebert, L., and Simkin, T.: *Volcanoes of the world: An Illustrated Catalog of Holocene Volcanoes and their Eruptions*, Smithsonian Institution, Global Volcanism Program Digital Information Series, GVP-3 (<http://www.volcano.si.edu/world/>), 2002.
- Silverman, B. W.: *Density Estimation*. London: Chapman and Hall, 1986.
- Spinei, E., Carn, S. A., Krotkov, N. A., Mount, G. H., Yang, K., and Krueger, A. J.: Validation of Ozone Monitoring Instrument SO₂ measurements in the Okmok volcanic cloud over Pullman, WA in July 2008, *J. Geophys. Res.*, 115, D00L08, doi:10.1029/2009JD013492, 2010.
- Strahan, S.E., and Douglass, A.R.: Evaluating the credibility of transport processes in simulations of ozone recovery using the Global Modeling Initiative three-dimensional model. *J. Geophys. Res.*, 109, D05110, doi:10.1029/2003JD004238, 2004.
- Streets, D. G., Yan, F., Chin, M., Diehl, T., Mahowald, N., Schultz, M., Wild, M., Wu, Y., and Yu, C.: Anthro-

- 675 pogenic and natural contributions to regional trends in aerosol
optical depth, 19802006, *J. Geophys. Res.*, 114, D00d18,
doi:10.1029/2008jd011624, 2009.
- Taubman, B. F., Hains, J. C., Thompson, A. M. , Marufu, L. T.,
Doddridge, B. G., Stehr, J. W., Piety, C. A. and Dickerson,
680 R.R.: Aircraft vertical profiles of trace gas and aerosol pol-
lution over the mid-Atlantic United States: Statistics and me-
teorological cluster analysis, *J. Geophys. Res.*, 111, D10S07,
doi:10.1029/2005JD006196, 2006.
- United States Environmental Protection Agency. (2010). Retrieved
685 from the EPA website: <http://www.epa.gov/ttn/airs/airsaqs/>.
- United States Environmental Protection Agency. (2011).
Retrieved from the EPA Air Quality System website:
<http://www.epa.gov/air/sulfurdioxide/>.
- 690 Ware, J. H., B. G. Ferris Jr., D. W. Dockery, J. D. Spengler, D. O.
Stram, F. E. Speizer, Effects of ambient sulfur oxides and sus-
pended particles on respiratory health of preadolescent children,
Am. Rev. Respir. Dis., 5, 834842, 1986.